Robotic Redearch

Abstract

Extensive work has been done in the singularity analysis of the 3-R$\underline{P}$R manipulator [79, 154, 155, 156]. Three types of singularities may exist for PMs [79]. For the analytic 3-R$\underline{P}$R planar PPM, architecture singularities are well known and can be easily avoided, and inverse kinematic singularities are known to happen at the boundary of the Cartesian workspace. The forward kinematic singularities (also type II or uncertainty singularities) are more elusive to geometric analysis and have been investigated in detail in [154, 155, 156]. The 3-R$\underline{P}$R PMs are classified into three classes according to the types of singularity loci in Cartesian workspace [154, 155]. The first is the 3-R$\underline{P}$R manipulators, such as the general case, for which the singular loci for a given orientation of the moving platform can be either a hyperbola, an ellipse, or a parabola. The second is the 3-R$\underline{P}$R manipulators, such as the 3-R$\underline{P}$R manipulator with aligned platforms, for which the singularity loci for a given orientation of the moving platform always form a hyperbola. The third is the 3-R$\underline{P}$R manipulators, such as the 3-R$\underline{P}$R manipulator with symmetrical aligned platforms, for which the singularity loci for a given orientation of the moving platform form a straight line. In [156], the singularity analysis of the 3-R$\underline{P}$R manipulator is performed using the Clifford algebra of the projective plane. In [41], it is shown using numerical examples that for a 3-R$\underline{P}$R manipulator with similar aligned platforms, the four solutions to its FDA fall into different singularity-free regions respectively. The uniqueness domains of the general 3-R$\underline{P}$R PPM is introduced and studied in [157]. It is also revealed that singularity-free trajectory-planning is time-consuming for the general case.

This section aims at revealing the relationship between the solutions in analytic form and the different singularity-free regions for 3-R$\underline{P}$R manipulator with similar platforms

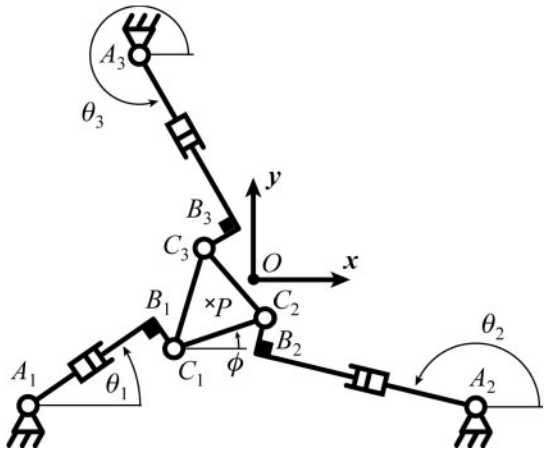

Fig. 1. Schematic representation of the 3-*RPR* planar parallel robot under study.

2. Kinematics and Singularity Analysis

The following analysis is based on the schematics of the robot shown in Figure 1. The revolute joints A_i ($i = 1, 2, 3$) are fixed on the base and are actuated. Each leg is composed of one passive prismatic joint, placed between points A_i and B_i, and one passive revolute joint C_i, connected to the mobile platform.

We consider that we control the position (x, y) of point P from the mobile platform and the orientation ϕ of the mobile platform. The origin of the base frame is chosen at point O. Points O and P are located at the centers of the circumscribed circles of triangles $A_1A_2A_3$ and $C_1C_2C_3$, respectively (Figure 2). Finally, let $\rho_i = |A_iB_i|$ and $L_i = |B_iC_i|$, the latter referred to as an *offset*.

It is therefore possible to express the position of points A_i and C_i as

$$\mathbf{OA}_i = \begin{bmatrix} x_{A_i} \\ y_{A_i} \end{bmatrix} = R_b \begin{bmatrix} \cos\gamma_i \\ \sin\gamma_i \end{bmatrix},$$

$$\mathbf{OC}_i = \begin{bmatrix} x_{C_i} \\ y_{C_i} \end{bmatrix} = \begin{bmatrix} x \\ y \end{bmatrix} + R_p \begin{bmatrix} \cos(\phi + \delta_i) \\ \sin(\phi + \delta_i) \end{bmatrix} \quad (1)$$

where $\gamma_i = (\alpha_b + \pi, -\alpha_b, -\alpha_b + \beta_b)$ and $\delta_i = (\alpha_p + \pi, -\alpha_p, -\alpha_p + \beta_p)$. From these expressions and referring to Bonev et al. (2003), one can determine the closure equations of the system:

$$\mathbf{OC}_i - \mathbf{OB}_i = \begin{bmatrix} x_{C_i} - x_{A_i} - \rho_i\cos\theta_i \\ y_{C_i} - y_{A_i} - \rho_i\sin\theta_i \end{bmatrix} = L_i \begin{bmatrix} -\sin\theta_i \\ \cos\theta_i \end{bmatrix}. \quad (2)$$

Refer to Bonev et al. (2003) for the full derivation. The velocity equation for the 3-*RPR* robot is:

$$\mathbf{A}\left[\dot{\phi}, \dot{x}, \dot{y}\right]^T = \mathbf{B}\left[\dot{\theta}_1, \dot{\theta}_2, \dot{\theta}_3\right]^T \quad (3)$$

with

$$\mathbf{A} = \begin{bmatrix} \mathbf{f}_1^T\mathbf{E}\mathbf{g}_1 & \mathbf{f}_1^T \\ \mathbf{f}_2^T\mathbf{E}\mathbf{g}_2 & \mathbf{f}_2^T \\ \mathbf{f}_3^T\mathbf{E}\mathbf{g}_3 & \mathbf{f}_3^T \end{bmatrix}, \quad \mathbf{B} = \begin{bmatrix} \rho_1 & 0 & 0 \\ 0 & \rho_2 & 0 \\ 0 & 0 & \rho_3 \end{bmatrix}, \quad (4)$$

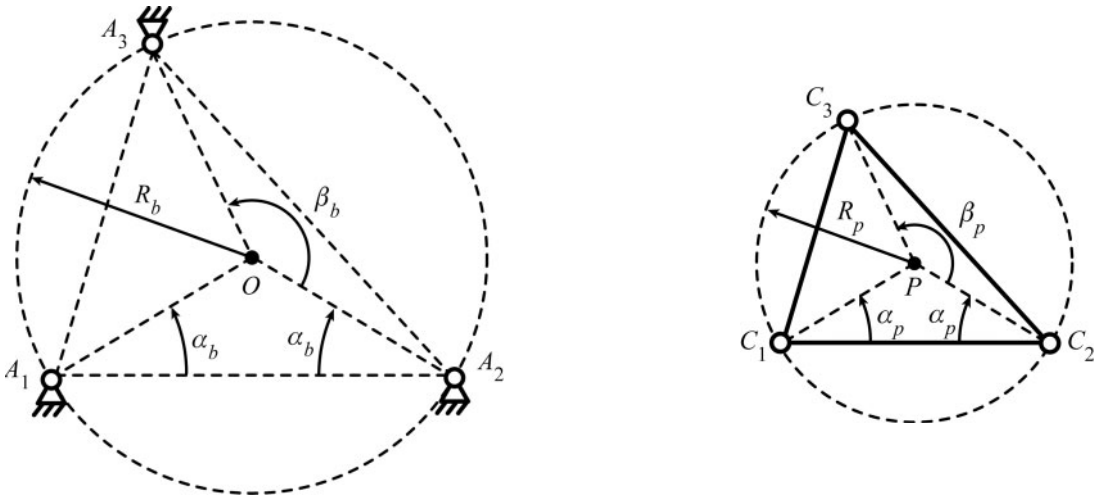

Fig. 2. Parameterization of the base and platform triangles: (a) fixed base and (b) mobile platform.

and

$$\mathbf{g}_i = \begin{bmatrix} x_{C_i} - x & y_{C_i} - y \end{bmatrix}^T, \quad \mathbf{E} = \begin{bmatrix} 0 & 1 \\ -1 & 0 \end{bmatrix},$$

$$\mathbf{f}_i = \begin{bmatrix} -\sin\theta_i \\ \cos\theta_i \end{bmatrix}. \tag{5}$$

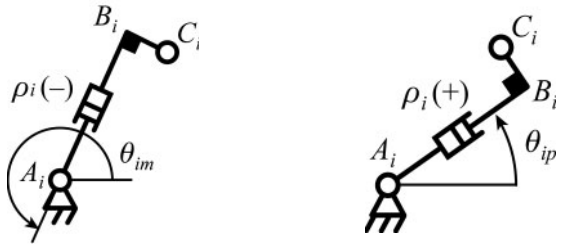

Fig. 3. The two inverse kinematic solutions of the *i*th leg of the robot: (a) first solution, ρ_i (+) and (b) second solution, ρ_i (–).

2.1. Inverse kinematic problem

Solving the inverse kinematics for each leg of this robot is essentially finding the intersection points between two circles, one with diameter $|A_iC_i|$ centered at the middle of segment A_iC_i, and one with radius L_i centered at C_i. Pre-multiplying both sides of Equation (2) with the term $\mathbf{f}_i^T$, one can obtain an equation expressing the angles θ_i as a function of the other parameters:

$$(x_{C_i} - x_{A_i})\sin\theta_i - (y_{C_i} - y_{A_i})\cos\theta_i - L_i = 0. \tag{6}$$

From Equation (6), it is possible to find the expressions for the active-joint variables θ_i as functions of the position (x, y) and the orientation ϕ of the mobile platform:

$$\theta_{ip} = 2\tan^{-1}\left(\frac{-(x_{Ci}-x_{Ai})+\sqrt{(x_{Ci}-x_{Ai})^2+(y_{Ci}-y_{Ai})^2-L_i^2}}{-L_i+y_{Ci}-y_{Ai}}\right), \tag{7a}$$

$$\theta_{im} = 2\tan^{-1}\left(\frac{-(x_{Ci}-x_{Ai})-\sqrt{(x_{Ci}-x_{Ai})^2+(y_{Ci}-y_{Ai})^2-L_i^2}}{-L_i+y_{Ci}-y_{Ai}}\right). \tag{7b}$$

The two solutions θ_{ip} and θ_{im} define the two inverse kinematic solutions for leg i (Figure 3). These define a total of eight solutions to the inverse kinematics of the parallel robot, also called *working modes* (Wenger and Chablat 1998). We will see that for this robot, provided there are non-zero offsets $L_i > 0$, the singularity loci will depend on the working mode.

2.2. Type 1 Singularities

Type 1 singularities occur when the determinant of **B** vanishes, i.e. when $\rho_i = 0$ (for i = 1, 2, or 3) (Figure 4) (Bonev et al. 2003). These configurations correspond to the internal boundaries of the workspace of a general 3-*RPR* planar parallel robot. When the offsets are zero, i.e. $L_i = 0$, there is a generic Type 1 (RI) singularity where the input velocities are indeterminate (Zlatanov et al. 1994). On this singularity, the inverse kinematic model of leg i admits only one solution because $(x_{Ci} - x_{Ai})^2 + (y_{Ci} - y_{Ai})^2 - L_i^2 = \rho_i^2 = 0$.

2.3. Direct Kinematic Problem

It is shown in Merlet (1996) that the solution of the direct kinematics of a 3*RPR* planar parallel robot is equivalent to finding

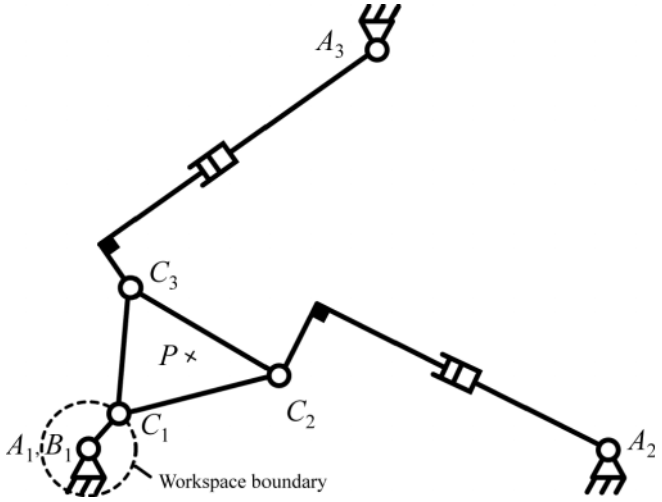

Fig. 4. Type 1 singularity.

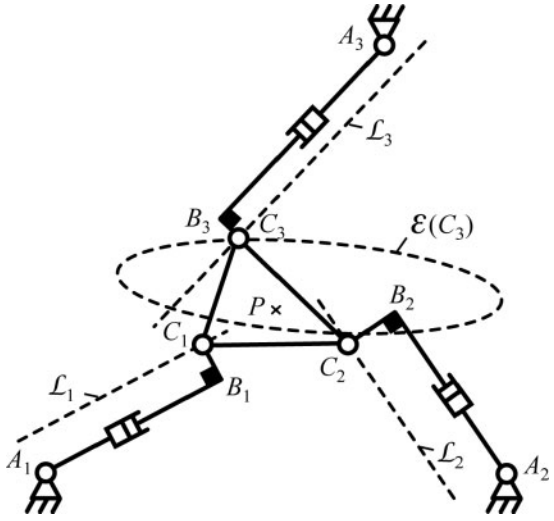

Fig. 5. Geometric interpretation of the direct kinematics.

the intersection points between an ellipse and a line, but no analytical expressions are given. Let us dismount the revolute joint at C_3. For given active-joint variables θ_1 and θ_2, points C_1 and C_2 are constrained to move along two lines, $\mathcal{L}_1$ and $\mathcal{L}_2$, respectively, and the mobile platform undergoes a Cardanic motion (Sekulie 1998; Tischler et al. 1998) (Figure 5). As a result, any points Q from the mobile platform, including P and C_i, describe a curve $\mathcal{E}(Q)$, which can be an ellipse, two parallel lines or a doubly-traced line segment. Thus, the direct kinematics can be solved by finding the intersection points between the curve $\mathcal{E}(C_3)$ and the line $\mathcal{L}_3$.

Let us now derive the expression of the elliptic curve $\mathcal{E}(C_3)$. It is possible to write the following closure equation:

$$\mathbf{OC}_3 = \mathbf{OA}_1 + \mathbf{A}_1\mathbf{B}_1 + \mathbf{B}_1\mathbf{C}_1 + \mathbf{C}_1\mathbf{C}_3. \tag{8}$$

This yields the expression:

$$\mathbf{OC}_3 = \begin{bmatrix} x_{C3} \\ y_{C3} \end{bmatrix} = \begin{bmatrix} x_{A1} \\ y_{A1} \end{bmatrix} + \rho_1 \begin{bmatrix} \cos\theta_1 \\ \sin\theta_1 \end{bmatrix} + L_1 \begin{bmatrix} -\sin\theta_1 \\ \cos\theta_1 \end{bmatrix} + 2R_p \cos\left(\frac{\beta_p}{2} - \alpha_p\right) \begin{bmatrix} \cos\left(\frac{\beta_p}{2} + \phi\right) \\ \sin\left(\frac{\beta_p}{2} + \phi\right) \end{bmatrix}. \tag{9}$$

In this expression, all parameters are known except ρ_1 and ϕ. However, they are dependent on each other. Without loss of generality, we choose ϕ as the independent variable and express ρ_1 as a function of ϕ, using the closure equation:

$$\mathbf{A}_1\mathbf{A}_2 = \mathbf{A}_1\mathbf{B}_1 + \mathbf{B}_1\mathbf{C}_1 + \mathbf{C}_1\mathbf{C}_2 + \mathbf{C}_2\mathbf{B}_2 + \mathbf{B}_2\mathbf{A}_2. \tag{10}$$

Developing this relation, we obtain:

$$\begin{bmatrix} x_{A2} - x_{A1} \\ y_{A2} - y_{A1} \end{bmatrix} = \rho_1 \begin{bmatrix} \cos\theta_1 \\ \sin\theta_1 \end{bmatrix} + L_1 \begin{bmatrix} -\sin\theta_1 \\ \cos\theta_1 \end{bmatrix} + 2R_p \cos\alpha_p \begin{bmatrix} \cos\phi \\ \sin\phi \end{bmatrix} - L_2 \begin{bmatrix} -\sin\theta_2 \\ \cos\theta_2 \end{bmatrix} - \rho_2 \begin{bmatrix} \cos\theta_2 \\ \sin\theta_2 \end{bmatrix}. \tag{11}$$

Expressing ρ_1 and ρ_2 as a function of ϕ from Equation (11), we obtain:

$$\rho_j = a_{j1} + a_{j2}\cos\phi + a_{j3}\sin\phi, \quad (j = 1, 2) \tag{12}$$

where the expressions for a_{ji} are given in the appendix. Substituting Equation (12) into Equation (9), we find the relation:

$$\mathbf{OC}_3 = \begin{bmatrix} x_{C3} \\ y_{C3} \end{bmatrix} = \begin{bmatrix} b_{11} + b_{12}\cos\phi + b_{13}\sin\phi \\ b_{21} + b_{22}\cos\phi + b_{23}\sin\phi \end{bmatrix}, \tag{13}$$

where b_{ji} $(j = 1, 2)$ are given in the appendix.

Therefore, for any fixed input parameters θ_i, we have found in Equation (13) the parametric expression of the elliptic curve $\mathcal{E}(C_3)$ depending on the orientation ϕ of the platform. Furthermore, we know that point C_3 belongs to line $\mathcal{L}_3$ with expression:

$$y = \tan\theta_3(x + L_3\sin\theta_3 - x_{A3}) + y_{A3} + L_3\cos\theta_3. \tag{14}$$

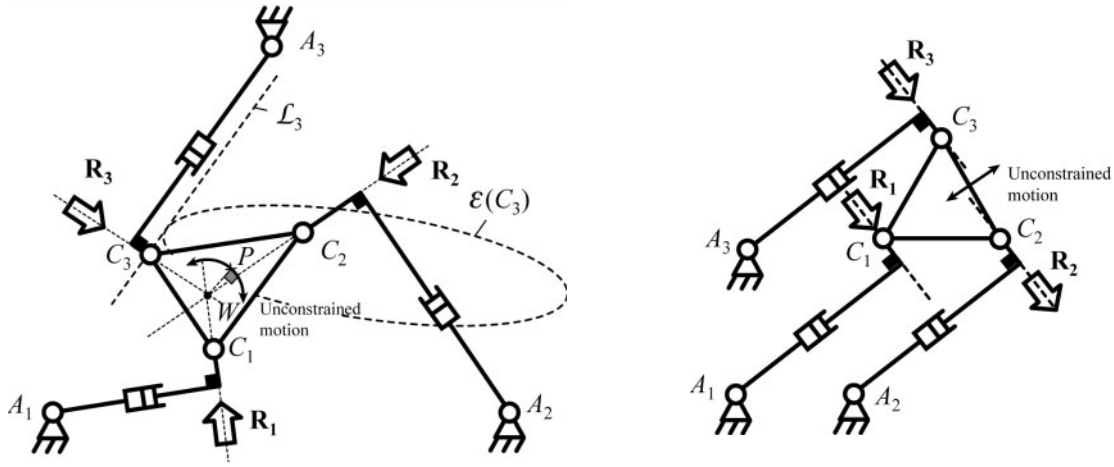

Fig. 6. Type 2 singularities of the parallel robot: (a) infinitesimal rotation about W and (b) finite translation (self-motion) along the direction of the prismatic joints.

Thus, the intersections between $\mathcal{E}(C_3)$ and $\mathcal{L}_3$ can be found by substituting x and y in Equation (14) by the expressions of x_{C3} and y_{C3} of Equation (13). After the substitution into Equation (14) and multiplying the equation by $\cos\theta_3$, we obtain:

$$\begin{aligned} 0 &= \sin\theta_3(x_{C3} + L_3\sin\theta_3 - x_{A3}) \\ &+ \cos\theta_3(y_{A3} + L_3\cos\theta_3 - y_{C3}). \end{aligned} \tag{15}$$

Developing Equation (15),

$$c_1 + c_2\cos\phi + c_3\sin\phi = 0, \tag{16}$$

where c_i are given in the appendix. From Equation (16), it is therefore possible to find the solution for ϕ:

$$\phi = 2\tan^{-1}\left(\frac{-c_3 \pm \sqrt{c_3^2 - c_1^2 + c_2^2}}{c_1 - c_2}\right). \tag{17}$$

Note that this solution is not unique and corresponds to the two assembly modes of the robot. Finally, it is possible to find the expression for the position using the closure equation:

$$\mathbf{OP} = \mathbf{OA}_1 + \mathbf{A}_1\mathbf{B}_1 + \mathbf{B}_1\mathbf{C}_1 + \mathbf{C}_1\mathbf{P} \tag{18}$$

which yields:

$$\begin{aligned} \mathbf{OP} &= \begin{bmatrix} x \\ y \end{bmatrix} = \begin{bmatrix} x_{A1} \\ y_{A1} \end{bmatrix} + \rho_1 \begin{bmatrix} \cos\theta_1 \\ \sin\theta_1 \end{bmatrix} \\ &+ L_1 \begin{bmatrix} -\sin\theta_1 \\ \cos\theta_1 \end{bmatrix} + R_p \begin{bmatrix} \cos(\phi + \alpha_p) \\ \sin(\phi + \alpha_p) \end{bmatrix}. \end{aligned} \tag{19}$$

2.4. Type 2 Singularities Analysis

Type 2 singularities occur when the determinant of **A** vanishes. It can be shown that the numerator of the determinant of matrix **A** contains three radicals and is dependent on the working mode. If we manipulate this expression properly and raise it to square three times, we can obtain a polynomial of degree 16 in x and y (Bonev et al. 2003). This polynomial will cover all working modes. Note, however, that if $L_i = 0$, the numerator becomes a quadratic polynomial in x and y and that the denominator of this expression is equal to $\rho_1\rho_2\rho_3$. Unfortunately, the study of this determinant cannot characterize the motion gained by the mobile platform at Type 2 singularities.

In a Type 2 singularity, the lines normal to the directions of the prismatic joints passing through points C_i are concurrent or parallel (Figure 6) (Bonev et al. 2003). These lines coincide with the direction of the forces $\mathbf{R}_i$ applied to the platform by the actuators.

However, we need more information for characterizing the complete kinematic behavior of the robot inside such a singular configuration. This can be found by studying the degeneracy of the direct kinematic model. Thus, there are Type 2 singularities if the following holds.

1. $\mathcal{E}(C_3)$ is an ellipse tangent to $\mathcal{L}_3$: in such a case, the directions of the three forces R_i intersect at one point W and the robot gains one infinitesimal rotation about this point (Figure 6a).

2. $\mathcal{L}_1$, $\mathcal{L}_2$ and $\mathcal{L}_3$ are parallel and $\mathcal{E}(C_3)$ degenerates to two lines parallel to $\mathcal{L}_1$ and $\mathcal{L}_2$ (and $\mathcal{L}_3$): in such a case, the directions of the three forces R_i are parallel and the robot gains one self-motion of translation (Figure 6b).